Luminescence of KCl single crystals doped with Ge atoms

1995 J. Phys.: Condens. Matter 7 7387

(http://iopscience.iop.org/0953-8984/7/37/011)

J. Phys.: Condens. Matter 7 (1995) 7387–7396. Printed in the UK

Luminescence of KCl single crystals doped with Ge atoms

Jun-Gill Kang†, So-Kyung Ju, Seoung-Won Lee‡ and Youn-Doo Kim
Department of Chemistry, Chungnam National University, Daejeon 305-764, South Korea

Received 23 February 1995, in final form 9 May 1995

Abstract. The emission from KCl:Ge^0 excited in the UV range was measured as a function of the exciting photon energy and temperature. The polarized emission spectrum and the angular dependence of polarization ratio were also investigated. Like KCl:Bi^{3+}, KCl:Ge^0 single crystals produce two emission bands peaking at 345 and 395 nm.

The interstitial Cl^- ion is assumed to be responsible for the colour centre of the 345 and 395 nm emissions. The definitive assignment of these bands is presented in terms of the adiabatic potential energy surface, in which the Jahn–Teller effect is taken into account.

1. Introduction

Previously, we reported A-band emission from divalent Ge ions in KCl single crystals (Kang *et al* 1988). The phosphor excited within the A absorption band produces complex emission bands (peaking at 345, 395, 515 and 675 nm). Those results are very abnormal, compared with two from Tl^+-like ions (Fukuda 1970). We assumed that the complex emission spectra could arise from various states of germanium present in the KCl crystal. This is very likely, since the KX:Ge^{2+} phosphor has usually been grown according to the stoichiometric redox reaction between Ge and GeX_4 at the crystal growth temperature. If germanium is present in its divalent state, the ion has an s^2 electronic configuration and the A-band excitation generally produces one or two emission bands. The analysis of the observed A-band emission from KCl:Ge^{2+} suggested that the two low-energy bands could be attributed to divalent Ge ions and the high-energy emission bands to other centres associated with Ge^0.

To date, the luminescence of Ge^0-like phosphors with a p^2 electronic configuration has not been reported. The two high-energy emission bands of KCl:Ge^{2+}, peaking at 345 and 395 nm, has not been clearly defined. These two emission bands have also been observed in KCl:Bi^{3+}, when the crystals are excited in the X absorption band located between the A and B absorption bands (Kim and Kang 1994). For KCl:Bi^{3+}, these two emission bands differ entirely from the two A emission bands (peaking at 388 and 430 nm). It is very likely that the perturbation arising from the substitution of impurity ions of relatively small size could cause one of the six Cl^- ions surrounding the substituted dopant cation to be in the interstitial position. For KCl:Bi^{3+}, the X-band emission has been attributed to an interstitial (or a loosely bonded) Cl^- ion.

The present work was undertaken to measure the luminescence of KCl crystals doped with Ge atoms as a function of the exciting photon energy and temperature and also

† Author to whom all correspondence should be addressed.
‡ Present address: LG Electronics Research Centre, 16 Woomyeon-Dong, Seocho-Gu, Seoul 137-140, South Korea.

0953-8984/95/377387+10$19.50

to investigate the polarization of the luminescence. In this paper, we report the optical characteristics of the phosphor in detail and confirm a possible model for interstitial Cl^- in KCl single crystals.

2. Experimental details

KCl:Ge^0 single crystals were grown from KCl powder containing about 300 ppm Ge^0 powder under vacuum using the vertical Bridgman method. Thin samples, cleaved from the ingot, were annealed at 500 °C for 1 h and then rapidly quenched to room temperature using the Cu block. The emission measurement at various temperatures was performed in an Air-Product He refrigerator using an APD-B temperature controller. Details of the optical arrangements for the emission measurement have been given in previous publication (*Kang et al* 1988).

The angular dependence of polarization at liquid-nitrogen temperature was also measured in an Oxford CF-1104 cryostat. Light from a 1000 W Xe arc lamp was passed through a Jobin–Yvon H-20 monochromator, followed by a UG-5 filter to improve further the monochromaticity of the excitation light. The excitation beam was linearly polarized using a Glan–Thomson prism polarizer in a rotatable mount. The polarization in the emitted radiation was measured at right angles to the incident beam using an analyser, consisting of a Glan–Thomson polarizer and a quartz quarter-wave plate. Measurement of the polarization in the parallel optical arrangement was also attempted. In this case, an appropriate band filter was placed before the sample to reduce the stray light. At a given angle of the polarizer with respect to the z axis denoted by α, two emission intensities were recorded: one with the analyser set at $\beta = \alpha$ from the z axis and the other with $\beta = \alpha + \pi/2$ from the z axis. Details of the optical arrangements have been given in a previous publication (Choi *et al* 1991).

3. Results

Measurement of the absorption spectrum at various temperatures was attempted. KCl:Ge^0, however, does not produce any characteristic absorption bands in the UV-visible wavelength range. KCl highly doped with Ge^0 may be required to attain the absorption spectrum.

The emission spectrum of thermally unquenched KCl single crystals doped with Ge^0 was measured at 33 K. As shown in figure 1, the 277 nm (4.48 eV) excitation produced two characteristic emission bands, peaking at 345 nm with a weak intensity and 395 nm with a strong intensity. An additional band appeared with a very weak intensity in the region of 450–650 nm. After the crystals were thermally annealed, the 345 and 395 nm emission bands were not changed at all, while the additional band on the low-energy side was not observed. This result suggests that the additional emission band may result from an aggregated state of colour centres in KCl.

The intensity spectrum of the emission from KCl:Ge^0 was measured at 78.8 K as a function of the exciting photon energy. The emission spectrum was found to be very affected by the exciting photon energy. The 250 nm excitation produces only the 395 nm emission band. On decreasing the exciting photon energy the intensity of the 395 nm emission increased and the 345 nm emission band was not produced up to 270 nm excitation. Upon 270 nm excitation, strong low-energy emission accompanied the weak high-energy emission peaking at 345 nm. The high-energy emission appeared only as a trace on 280 nm excitation. The excitation spectrum of these two emissions was measured at 78.8 K. As

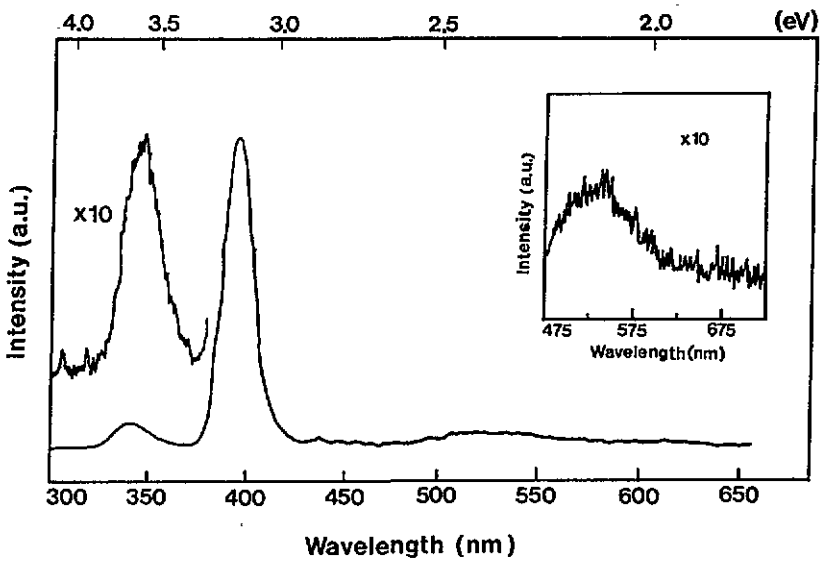

Figure 1. Emission spectrum from thermally unquenched KCl:Ge^0 excited at 277 nm (T = 33 K) (a.u., arbitrary units).

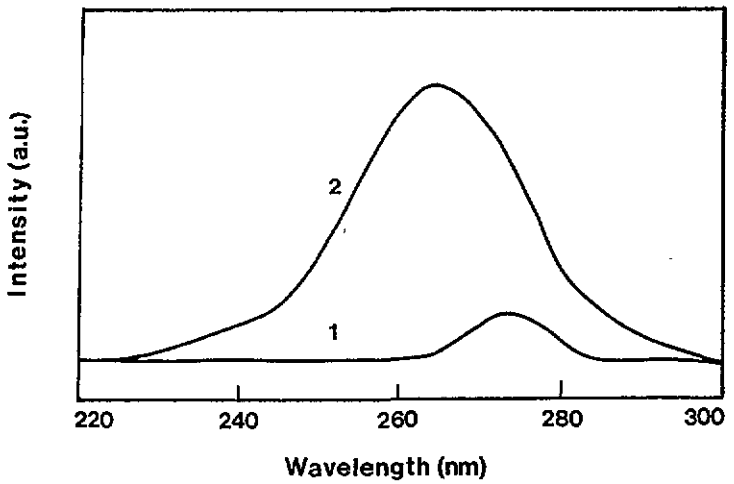

Figure 2. Excitation spectra of the 345 nm (curve 1) and the 395 nm (curve 2) emissions from KCl:Ge^0 (T = 78.8 K) (a.u., arbitrary units).

shown in figure 2, the excitation spectra for both emissions differ entirely in peak position and bandwidth. For the 395 nm emission the excitation spectrum peaking at 265 nm is ranged over 230–290 nm and its intensity is strong, while for the 345 nm emission the excitation spectrum peaking at 275 nm is very weak with narrow bandwidth. The excitation spectrum indicates that the emitting centres accountable for the two emissions are not identical.

The emission spectrum of KCl:Ge^0 single crystals was measured at various temperatures. With increasing temperature the intensity of the two bands decreased gradually but persisted to a certain extent up to room temperature. Their peak positions were found to be nearly independent of temperature. This indicates that thermal expansion of the crystal is negligible.

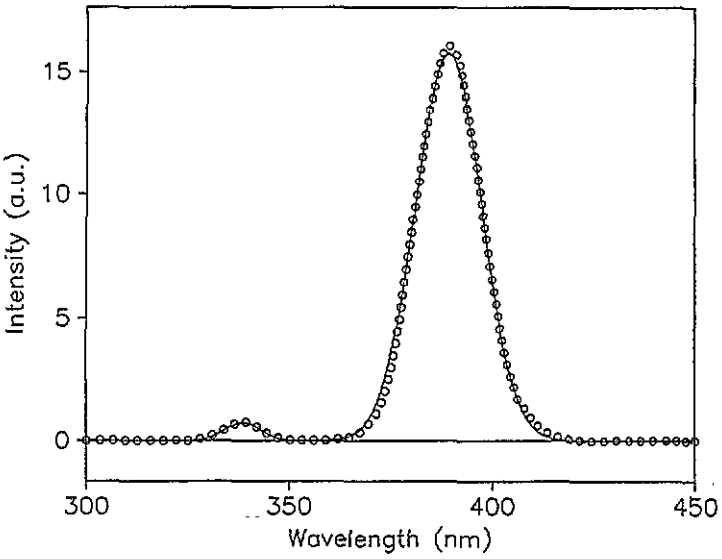

Figure 3. Resolution of the emission spectrum from KCl:Ge^0 excited at 277 nm ($T = 33$ K) (a.u., arbitrary units): ——, individual resolved bands and their sum; O, experimental data.

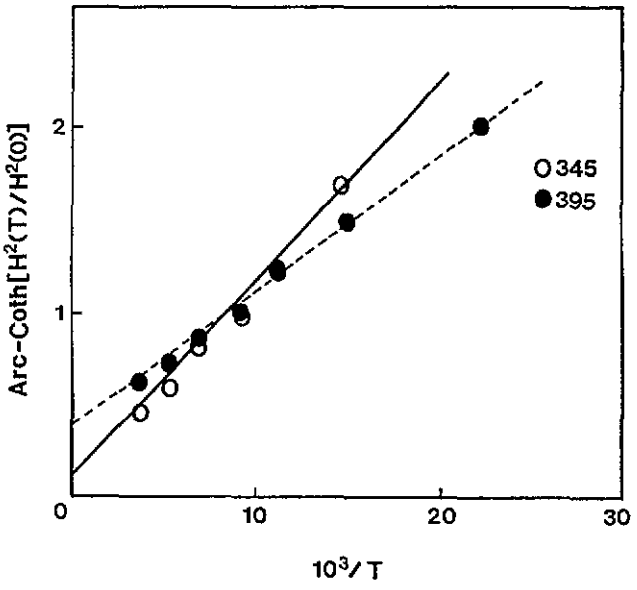

Figure 4. Arc hyperbolic cotangent plot of the 345 nm (O) and 395 nm (●) emission band half-widths versus the reciprocal of the temperature.

The deconvolution of the spectrum was performed using the Gaussian formula. Figure 3 shows the computer plot of a deconvoluted spectrum and the experimental data of the corresponding emission spectrum with background subtracted. Both of the two emissions consist of a single Gaussian band. Figure 4 is a plot of the half-width of the emission band versus the reciprocal temperature, which is described in the semiclassical approximation by $H^2(T) = H^2(0)\coth(h\nu/2kT)$. Here $H(0)$ is the half-width at $T = 0$ K which was

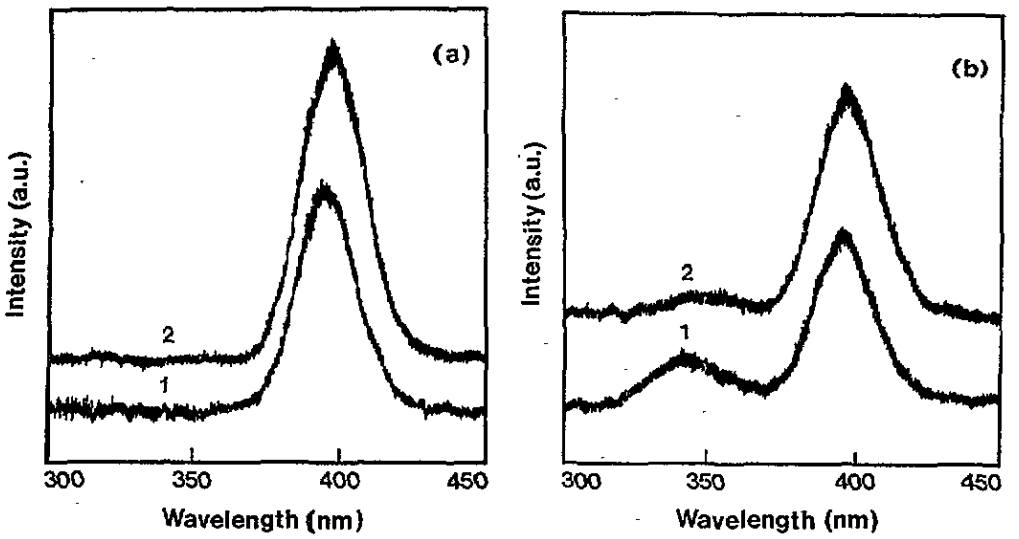

Figure 5. Polarized emission spectra from KCl:Ge^0 excited at (a) 264 nm and (b) 272 nm ($T = 78.8$ K) (a.u., arbitrary units): curves 1, the Π spectrum; curves 2, the Σ spectrum.

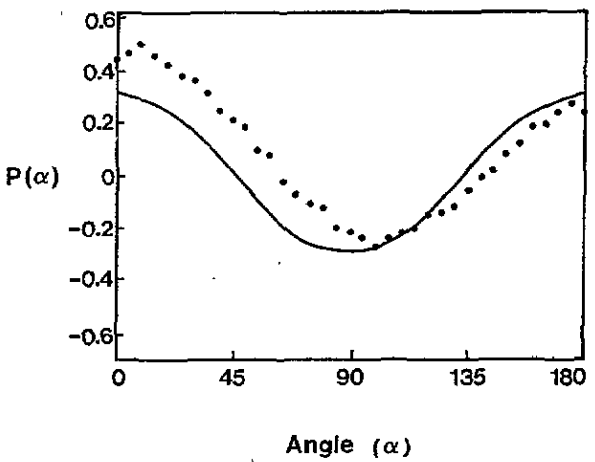

Figure 6. Angular dependence of the polarization ratio for the 345 nm emission from KCl:Ge^0 in the perpendicular optical geometry ($T = 78.8$ K): ——, calculated from $P(\alpha) = 0.3\cos(2\alpha)$. In the parallel geometry, the intensity was too low to obtain the polarization ratio, owing to the band filter placed before the sample in order to cut the unwanted stray light.

obtained by extrapolation of $H(T)$ to 0 K in the plot of $H(T)$ versus T. From the slope of figure 4, the average phonon frequencies for the 345 and 395 nm emitting centres are obtained as 3.67×10^{12} s^{-1} and 3.06×10^{12} s^{-1}, respectively. The temperature dependence of the two emission bands indicates that the linear electron–phonon interaction plays an important role in the emission process.

The intensity spectra of the 345 and 395 nm emissions from KCl:Ge^0 polarized parallel and perpendicular to the direction of the electric vector of the exciting light were also

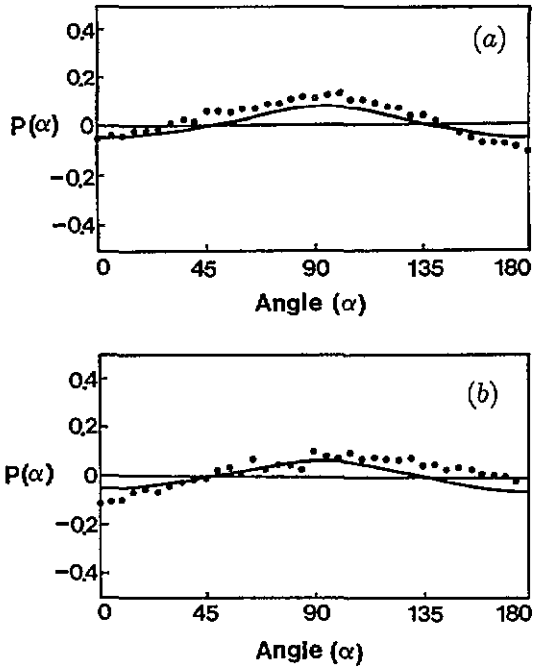

Figure 7. Angular dependence of the polarization ratio for the 395 nm emission from KCl:Ge^0 in (a) the parallel and (b) the perpendicular optical geometries ($T = 78.8$ K): ——, calculated from $P(\alpha) = -0.1\cos(2\alpha)$.

measured at 78.8 K. As shown in figure 5, for the 345 nm emission band the intensity (I_Π) polarized parallel is stronger than the intensity (I_Σ) polarized perpendicular while for the 395 nm emission the intensity of the Σ emission band is stronger than that of the Π emission band. It can be assumed that the absorbing and emitting states could be identical since no further splitting of the polarized emission spectra is observed. The angular dependence of the polarization ratio of the two emissions was also measured at 78.8 K in the perpendicular optical geometry. As shown in figure 6, for the 345 nm emission the polarization ratio P is a maximum when the exciting light is polarized at $\alpha = 0$ or 180° and P is a minimum at $\alpha = 90°$. It can be seen that $P(\alpha)$ of the 345 nm emission is proportional to $\cos(2\alpha)$. Figure 7 shows the angular dependence of the polarization ratio of the 395 nm emission measured in both the perpendicular and parallel geometries. Independently of the optical arrangement, P is a maximum at 90° and P is a minimum at $\alpha = 0$ or 180°. The values of $P(0°)$ and $P(90°)$, however, are very small so that the 395 nm emission can be assumed to be nearly depolarized, independently of the angle of the electric vector of the exciting light. The angular dependence of $P(\alpha)$ reveals that the dipoles responsible for the 345 and 395 nm emissions could be oriented along the C_4 and C_3 symmetry axes, respectively.

4. Discussion

First of all, the electronic states of Ge^0 under the crystal-field potential of O_h symmetry can be considerable for the assignment of the 345 and 395 nm emissions. For Ge^0 in KCl, the A-band absorption corresponds to transitions from the ground $^3A_{1g}(^3P_0)$ state to the excited

$^3T_{1u}(^3P_1)$ state. This transition is totally allowed by an electric dipole moment so that the A absorption band should be strongly observed like the C absorption band ($^1A_{1g} \rightarrow {}^1T_{1u}$) of Tl^+-type phosphors. Unfortunately, KCl:Ge^0 does not produce any allowed absorption bands in the UV–visible region. It could allow us to rule out the possibility that the 345 and 395 nm emissions originated from Ge^0 electronic states.

Except for the relative magnitudes of the intensities of the 345 and 395 nm emissions, all results observed for KCl:Ge^0 are the same as those for KCl:Bi^{3+}. This similarity for the 345 and 395 nm emissions leads us to confirm the model proposed previously, in which a perturbation arising from substitution of an impurity ion of small size was taken into account (Kim and Kang 1994). Here, it should be noted that the excitation energy of the 345 and 395 nm emissions is much higher than that of the V_K centre but much lower than the intrinsic transition of the Cl^- ion at the valence band.

When the Ge atom is incorporated into the lattice of KCl, interspacing may occur due to the small size of Ge atom (1.22 Å) compared with the ionic size of K^+ (1.33 Å). One of six neighbouring Cl^- ions may move into the interstitial position, resulting in lattice distortion. This interstitial Cl^- ion (hereafter referred to as $(Cl^-)^*$) could experience a reduced crystal-field potential with the symmetry C_{4v}. The reduced crystal-field potential may cause the electronic states of the $(Cl^-)^*$ to be trapped as a colour centre between the valence band and the conduction band. This centre may account for the 345 and 395 nm emissions from KCl single crystals doped with an impurity of small size.

The ground and first excited states of $(Cl^-)^*$ are $^1S_0$ and $^3P_2$, respectively. Under the C_{4v} crystal-field potential, the fivefold $^3P_2$ state is split into the non-degenerate $^3A_1$, $^3B_1$ and $^3B_2$ states and the twofold ^3E state. The $^1A_1 \rightarrow {}^3B_1$ and $^1A_1 \rightarrow {}^3B_2$ transitions are totally forbidden by an electric dipole moment but the $^1A_1 \rightarrow {}^3A_1$ and $^1A_1 \rightarrow {}^3E$ transitions are partially allowed by the orbital selection rule.

Previously, we proposed an energy-level scheme for the 345 and 395 nm emissions (Kim and Kang 1994). In this paper, we shall re-examine the $^3A_1$ and ^3E states for the precise assignment of the 345 and 395 nm emissions in terms of the Jahn–Teller effect (JTE). It should be noted that, for the $^3A_1$ and ^3E states, additional stabilization is not expected since the off-diagonal elements of spin–orbit interaction are zero. Among the 15 vibrational modes, the $a_1(Q_1)$, $b_1(Q_{b1})$, $b_2(Q_{b2})$ and $e(Q_\theta, Q_\epsilon)$ modes are active in the vibronic interactions.

For the $^3A_1$ state, Jahn–Teller (JT) stabilization would take place by the coupling with only the totally symmetric a_1 mode. For the ^3E state, the JT problem is specified by coupling to the a_1, b_1 and b_2 modes, since $E \times E = A_1 + A_2 + B_1 + B_2$. It can be seen that the JT stabilization is very significant in the relaxation process in the ^3E state, compared with the case of the $^3A_1$ state. The doubly degenerate E state can be significantly reduced by the JTE but this Kramers degeneracy is not removed. The JT problem of $E \otimes (b_1 + b_2)$ is well understood (Bacci 1978, Ballhausen 1965, Bersuker 1984). Here, we shall derive the adiabatic potential energy surface (APES) of the relaxed excited E state.

In the linear approximation, defining the JT coupling constants in terms of the operator of the vibronic interaction V_E as

$$F_{b_1} = -\langle E^x|\frac{\partial V_E}{\partial Q_{b_1}}|E^x\rangle = \langle E^y|\frac{\partial V_E}{\partial Q_{b_1}}|E^y\rangle$$

$$F_{b_2} = \langle E^x|\frac{\partial V_E}{\partial Q_{b_2}}|E^y\rangle$$

the JT stabilization on the APES is specified by

$$E_\pm(Q_{b_1}, Q_{b_2}) = \tfrac{1}{2}(K_{b_1}Q_{b_1}^2 + K_{b_2}Q_{b_2}^2) \pm (F_{b_1}^2 Q_{b_1}^2 + F_{b_2}^2 Q_{b_2}^2)^{1/2}$$

where K_Γ represents the force constant of the harmonic oscillator of the Γ mode and the first term on the right-hand side is the lattice energy. The lower solution E_- corresponds to the JT stabilization on the APES of the E state. The two extreme cases give rise to the well localized minima on the APES of the E state. When the coupling to the b_1 mode is much stronger than that to the b_2 mode, i.e. $F_{b_1}^2 \gg F_{b_2}^2$, a pair of rectangular minima exist at the point $(\pm F_{b_1}/K_{b_1}, 0)$ on the APES of the E state. Numerical analysis of the APES shows that the rectangular minima can move with the transforming character of $x^2 - y^2$ if $K_{b_2}/K_{b_1} > 0.2$ and $F_{b_2}^2/F_{b_1}^2 < 0.2$ (figure 8(a)). In the other extreme case, a pair of rhombic minima can be found at the point $(0, \pm K_{b_2}/F_{b_2})$. These minima move with the transforming character of xy if $K_{b_2}/K_{b_1} < 0.2$ and $F_{b_2}^2/F_{b_1}^2 > 0.2$ (figure 8(b)). For the particular case, where $F_{b_1}^2 \simeq F_{b_2}^2$, there is a continuum of minima along the bottom of the trough of the likely Mexican hat. In the linear JT coupling, two kinds of minima cannot coexist on the APES of the E state. In the intermediate case, where the coupling strengths of the b_1 and the b_2 modes are comparable with each other, the continuum of minima is favourable (figure 8(c)). In this case, the molecule can rotate freely between the rectangular and rhombic configurations. Here, the energy of the minima corresponds to the JT stabilization energy (e.g. $E_{\min} = -8530$ cm^{-1} for figure 8(c)). Assuming that E_{JT} is approximately half the Stokes shift, one can find that the JT stabilization energy for the 395 nm emission is about -6210 cm^{-1}. Comparing the calculated energy with the observed value, the relative strengths of the b_1 and the b_2 modes may be reasonable for the observed evidence.

Figure 9 shows the cross sections of the A and E states along any vertical plane involving the z axis. These configurational coordinate diagrams of the $^3A_1$ and ^3E states give a more definitive assignment of the X-band emission from the $(Cl^-)^*$ centre in KCl single crystals. The $^3A_1$ well can attain the maximum of the population via the excitation from the ground state to the point A and produces the 345 nm emission (referred to as X_{A_1}). Before reaching the point B, the ^3E well can attain the population via the tunnelling phenomenon. Upon excitation above the point B, the ^3E well may mainly attain the population and produce the strong 395 nm emission (referred to as X_E).

The polarization of the two emission bands may be indicative of the nature of the excited states. Here, we assume that the nature of polarization of the emitting light could be associated with the orbital itself. Upon excitation with polarized exciting light, the orientation of the emitting dipole is parallel to that of the absorbing dipole for the $A_1 \leftrightarrow A_1$ transitions, since the A_1 orbital is characterized by the spatial transformation along the z axis. Under this condition, the angular dependence of the polarization ratio can be formulated by $P(\alpha) \propto \cos(2\alpha)$. The observed results of the 345 nm emission obey this formula well.

For the ^3E state, not only are the minima characterized as of circular geometry but also the $A_1 \leftrightarrow E$ transitions are allowed by the (x, y)-polarized electric dipoles. For this case, the angular dependence of the polarization ratio of the 395 nm emission from the ^3E state may be specified by $P(\alpha) \propto -\cos(2\alpha)$ in both the [100]–[100] and [100]–[010] geometries. The observed results show only a trace of this angular dependence. The X_E emission could be nearly depolarized, independently of the vector of the exciting light. At this moment, the depolarization phenomenon of the 395 nm emission is not clearly solved. However, one of possible reasons could be the tunnelling effect; if some part of populations of the ^3E well is attained via tunnelling processes from the upper $^3A_1$ state to the lower ^3E state, the depolarization may appear in a part.

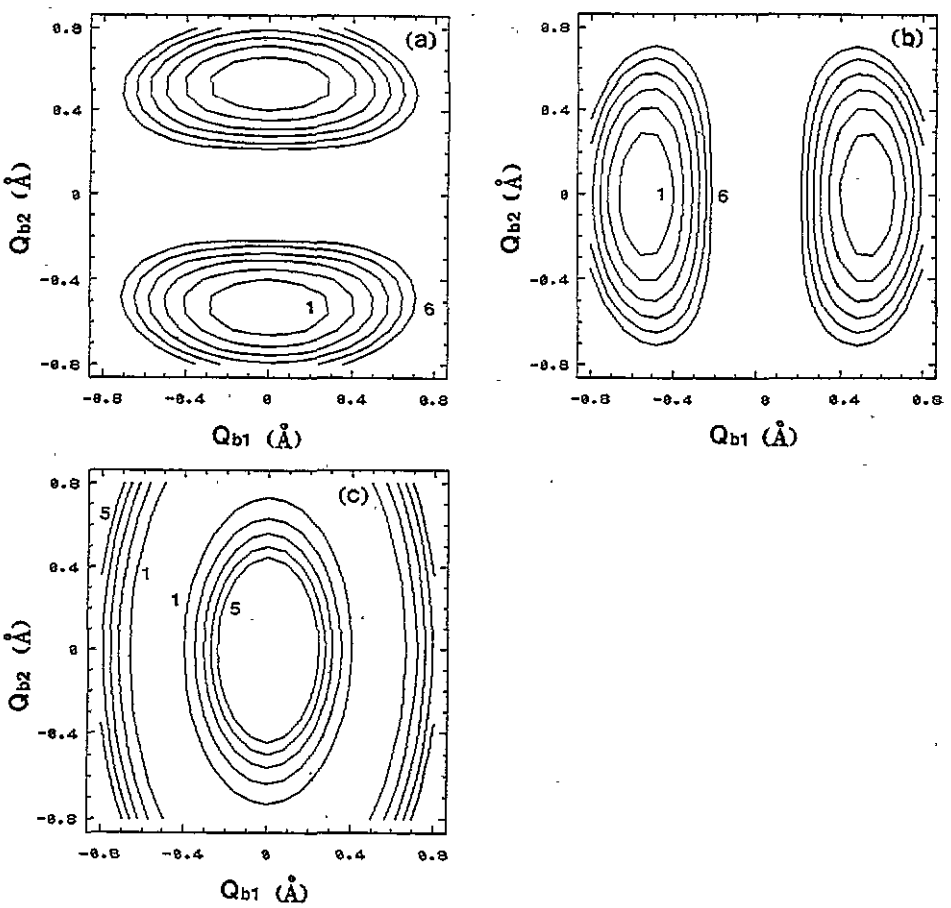

Figure 8. Contour of the APES of the E state. The maps in the $Q_{b_1}Q_{b_2}$ plane computed with (a) $K_{b_1} = 6.0 \times 10^4$ cm^{-1} Å^{-1}, $K_{b_2} = 1.8 \times 10^4$ cm^{-1} Å^{-1}, $F_{b_1} = 3.2 \times 10^4$ cm^{-1} Å^{-1} and $F_{b_2} = 1.0 \times 10^4$ cm^{-1} Å^{-1}, (b) $K_{b_1} = 1.8 \times 10^4$ cm^{-1} Å^{-1}, $K_{b_2} = 6.0 \times 10^4$ cm^{-1} Å^{-1}, $F_{b_1} = 1.0 \times 10^4$ cm^{-1} Å^{-1} and $F_{b_2} = 3.2 \times 10^4$ cm^{-1} Å^{-1} and (c) $K_{b_1} = 6.0 \times 10^4$ cm^{-1} Å^{-1}, $K_{b_2} = 2.4 \times 10^4$ cm^{-1} Å^{-1}, $F_{b_1} = 3.2 \times 10^4$ cm^{-1} Å^{-1} and $F_{b_2} = 1.8 \times 10^4$ cm^{-1} Å^{-1} show the rectangular, the rhombic and the somewhat continuum minima, respectively. Curve 1 represents -8000 cm^{-1} and the energy difference between the iso-energetic curves is 500 cm^{-1}.

5. Conclusions

When impurity ions of relatively small ion size are substituted into the lattice of KCl single crystals, interspacing could take place. This may give rise to an interstitial or loosely bonded Cl^- ion, referred to as $(Cl^-)^*$. Like KCl:Bi^{3+}, KCl:Ge^0 single crystals produce the 345 and 395 nm emission bands. These two bands are attributed to the $(Cl^-)^*$ centre.

For the precise assignment of these two emission bands, the electronic structure of the $(Cl^-)^*$ centre is investigated in the JTE. Under the reduced static potential of C_{4v}, the $^3A_1$ and ^3E states arising from the first exited $^3P_2$ term could account for the 345 and 395 nm emissions. For the $^3A_1$ state, the JTE coupling to the a_1 mode induces a totally symmetric distortion. On the contrary, for the ^3E state, the coupling to the b_1 and b_2 modes gives rise to the continuum of the minima on the APES with the transforming property of $(x^2 - y^2, xy)$. These considerations lead us to assign the 345 nm and 395 nm emission bands to transitions

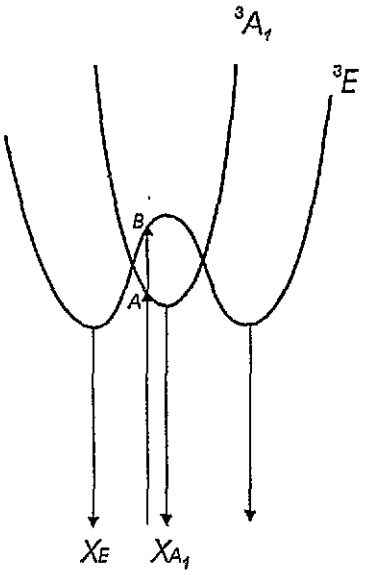

Figure 9. Configurational coordinate diagram for the relaxed excited $^3A_1$ and ^3E states of the $(Cl^-)^*$ centre, formulated in terms of the JT coupling to the A_1, B_1 and B_2 modes.

from the $^3A_1$ and ^3E states respectively, to the ground $^1A_1$ state.

The experimental evidence indicates that the nature of the impurity ion itself may not have an effect on the energy-level scheme of the $(Cl^-)^*$ centre but may do so on the optical transition probability via the overlapping of the eigenfunction between the ground and the excited states by the perturbed crystal-field potential.

Acknowledgments

This work was supported by the Non Directed Research Fund, Korea Research Foundation.

References

Bacci M 1978 *Phys. Rev.* B **17** 4495
Ballhausen C J 1965 *Theor. Chim. Acta* **3** 368
Bersuker I B 1984 *The Jahn-Teller Effect and Vibronic Interactions in Modern Chemistry* (New York: Plenum) ch 2
Choi K O, Lee S W, Bae H K, Jung S H, Chang C K and Kang J G 1991 *J. Chem. Phys.* **49** 6420
Fukuda A 1970 *Phys. Rev.* B **1** 4161
Kang J G, Ju S K, Gill Y H, Shim I K and Chang K 1988 *J. Phys. Chem. Solids* **49** 813
Kim Y D and Kang J G 1994 *J. Phys.: Condens. Matter* **6** 8949